The influence of ENSO on air-sea interaction in the Atlantic

Michael Alexander and James Scott
NOAA-CIRES Climate Diagnostics Center, USA

Received 7 November 2001; accepted 17 May 2002; published 27 July 2002.

[1] Observations and model experiments are used to investigate the influence of El Niño/the Southern Oscillation (ENSO) on air-sea interaction in the north Atlantic, Gulf of Mexico and Caribbean Sea. In one experiment, observed sea surface temperatures (SSTs) in the tropical Pacific are specified as boundary conditions in an atmospheric general circulation model (AGCM), while SSTs over the remainder of the global oceans are simulated by a mixed layer model. The observed warming in the tropical North Atlantic and cooling in the Gulf of Mexico in the winter/spring after ENSO peaks is well simulated by the model. Prior to the basin wide warming, latent heat fluxes generate negative SST anomalies in the Caribbean during August–October. Ocean-atmosphere coupling outside of the tropical Pacific significantly enhances the warm season atmospheric response to ENSO in the Caribbean region. *INDEX TERMS:* 4215 Oceanography: General: Climate and interannual variability (3309); 4522 Oceanography: Physical: El Niño; 4504 Oceanography: Physical: Air/sea interactions (0312); 3339 Meteorology and Atmospheric Dynamics: Ocean/atmosphere interactions (0312, 4504)

1. Introduction

[2] Atmospheric teleconnections associated with ENSO alter the air temperature, humidity, winds, and clouds, which can then generate SST anomalies far from the equatorial Pacific. The link between SST anomalies in the equatorial Pacific and those in the tropical Atlantic was first examined by *Covey and Hastenrath*, [1978] who found a broad region of warm SSTs to the north of the equator in boreal spring after El Niño peaks and roughly the opposite after La Niña events. These results were confirmed by subsequent observational analyses [e.g., *Curtis and Hastenrath*, 1995; *Enfield and Mayer*, 1997; *Klein et al.*, 1999]. Here, we investigate the evolution of ENSO-related SST anomalies in the north Atlantic and adjacent seas, the processes that generate the anomalies and the extent to which the SSTs feed back on the atmosphere.

2. Model Simulations

[3] We examine the ENSO-Atlantic relationship using 50 years of data (1950–1999) obtained from the National Center for Environmental Prediction (NCEP) reanalysis project and two sets of model experiments. In both sets of experiments, simulations are conducted using the GFDL R30 AGCM in which observed SSTs are specified in the eastern tropical Pacific (15°S–15°N, 172.5°E-South America) over the period 1950–1999. The two experiments only differ in their treatment of the ocean outside of this region. In the mixed layer model ("MLM") experiment, a one-dimensional mixed layer model was coupled to the AGCM at each gridpoint over the ice-free ocean outside of the tropical Pacific region. The ocean model simulates the mixed layer temperature (equivalent to SST), salinity and depth, but not currents and thus requires a flux correction to maintain a realistic climate. In the "Control" experiment, climatological SSTs, which repeat the same seasonal cycle each year, are specified at all ocean points beyond the tropical Pacific. The Control is often referred to as a "Tropical Ocean Global Atmosphere" or "TOGA" experiment in the literature. *Alexander et al.* [2002] described the experiment design in greater detail, while *Alexander and Scott* [1996] documented the AGCM's climate.

[4] The atmospheric response to the prescribed boundary conditions can drive SST anomalies outside the tropical Pacific in the MLM but not the Control experiment. Differences between the two experiments are used to study the extent to which air-sea interaction in the tropical Atlantic affects the atmospheric response to ENSO. To enhance the signal-to-noise ratio, experiments are performed using an ensemble of simulations, where each simulation is initiated with a different atmospheric state. All results presented here are from the ensemble averages of the 8 Control and 16 MLM simulations.

3. Results

[5] Composites are constructed based on 9 El Niño and 9 La Niña events during the 1950–1999 period. The El Niño events, as identified by *Trenberth* [1997], begin in 1957, 65, 69, 72, 76, 82, 87, 91, 97 and the La Niña events in 1950, 54, 55, 64, 70, 73, 75, 88, 98. Anomalies, defined here as the difference between the El Niño (warm) and La Niña (cold) composites, are presented in Figure 1 for sea level pressure (SLP) and surface winds during December–January–February (DJF 0/1) and SST during February–March–April (FMA 1), where 0 indicates the year ENSO peaks and 1 the following year. We chose these periods since atmospheric anomalies associated ENSO reach a maximum near the end of year(0) while most of the SST anomalies in the North Atlantic peak 2–5 months later [e.g., *Harrison and Larkin*, 1998].

[6] In both observations and the MLM experiment, a negative SLP anomaly extends across the North Atlantic with a southwest to northeast orientation. A positive SLP anomaly centered to the northeast of Brazil is associated with both the descending branch of the Walker Circulation and the atmospheric teleconnections that pass through the Pacific/North American sector [see Figure 9 in *Mestas-Nuñez and Enfield*, 2001]. The resulting negative SLP gradient from 5°N to 40°N weakens the trade winds in the

0094-8276/02/2001GL014347$05.00

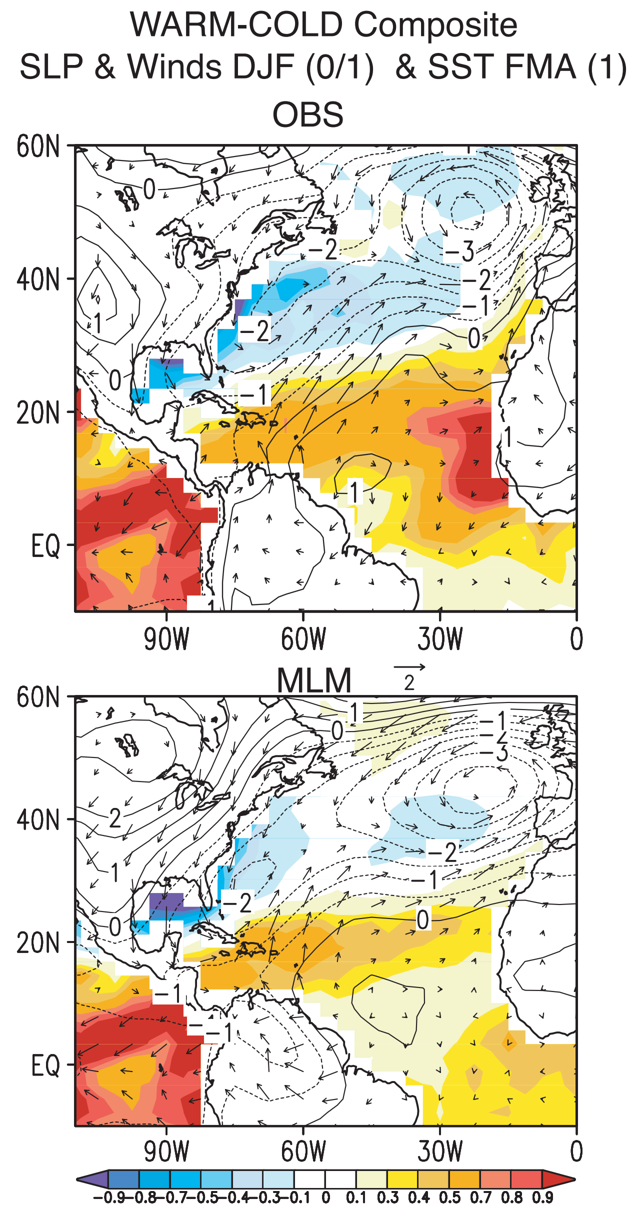

Figure 1. Observed (NCEP) and simulated (MLM) El Niño (warm) - La Niña (cold) composite of SLP (contour interval 1 mb) surface wind vectors (m sec^{-1}, scale beneath top panel) during DJF(0/1), and SST (shading interval of 0.1°C) during MAM (1) over the North Atlantic.

subtropics and strengthens the westerlies in the central North Atlantic. In addition, anomalous southward flow over the eastern U.S. advects cold continental air over the southern and eastern seaboard. Over the course of the winter, these changes in the atmospheric circulation generate cold water in the Gulf of Mexico/eastern north Atlantic and warm water in the north tropical Atlantic. The underestimation of the ENSO-related warming in the eastern half of the north tropical Atlantic in the MLM may be due to the absence of currents and upwelling and/or the overestimation of the mean mixed layer depth in this region. The latter causes the surface flux forcing to be distributed over a thicker layer resulting in smaller SST anomalies.

[7] In the model, atmospheric changes can influence SST via the surface heat flux and the entrainment of water into the mixed layer from below (vertical diffusion and penetrating solar radiation are included in the model by have a small impact on SSTs). The simulated SST anomalies that form in the Atlantic in late winter are primarily generated by the anomalous surface heat flux. Entrainment plays a secondary role in late winter but can be important at other times of the year. For example, temperature anomalies created in winter and then stored beneath the mixed layer in summer can be re-entrained into the surface layer in the following fall and early winter. As a result, SST anomalies that develop in the Gulf of Mexico in FMA(1) recur in the following winter (not shown). We have also diagnosed the role of Ekman transport in both observations and the MLM; it has a negligible impact on ENSO-related SSTs in the Atlantic except in a narrow region to the north of Columbia.

[8] Most previous studies emphasized the role of latent heat flux (Q_{lh}) anomalies in warming the tropical north Atlantic near the end of El Niño events [*Curtis and Hastenrath*, 1995; *Enfield and Mayer*, 1997; *Klein et al.*, 1999; *Saravanan and Chang*, 2000]. This is confirmed in the MLM where Q_{lh} anomalies are large in the eastern third of the basin between 15°N-20°N (Figure 2). However, other fluxes also affect the surface heat budget: shortwave radiation (Q_{sw}) is a dominant term between 5°N and 30°N, while the sensible heat flux (Q_{sh}) anomalies are about of equal importance as the latent fluxes in cooling the ocean along the U.S. coast (Figure 2). The longwave fluxes (Q_{lw}) are weak and tend to oppose the Q_{sw} values.

[9] The bulk formulas for Q_{sh} and Q_{lh} depend on the wind speed (U), and the air-sea difference in temperature (ΔT) and specific humidity (Δq), respectively. Splitting the atmospheric variables into their time mean ($\bar{\ }$) and

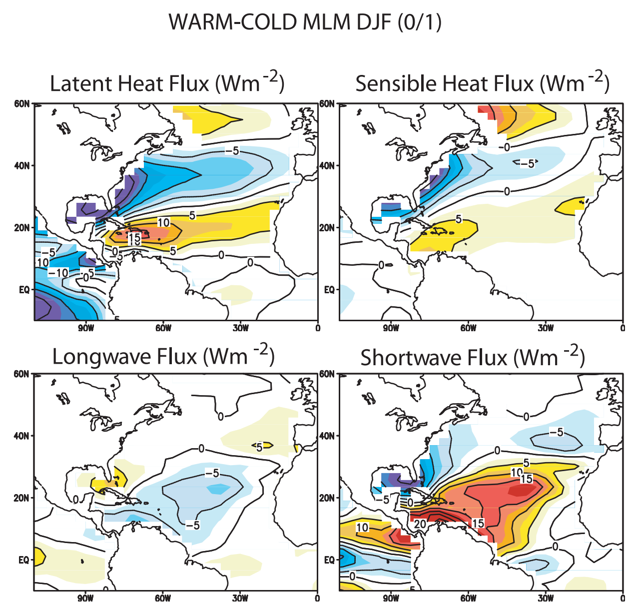

Figure 2. The El Niño - La Niña composite of the four surface heat flux components (contour interval 5 W m^{-2}) during DJF (0/1) from the MLM experiment. The fluxes have been smoothed in space using a 9-point filter.

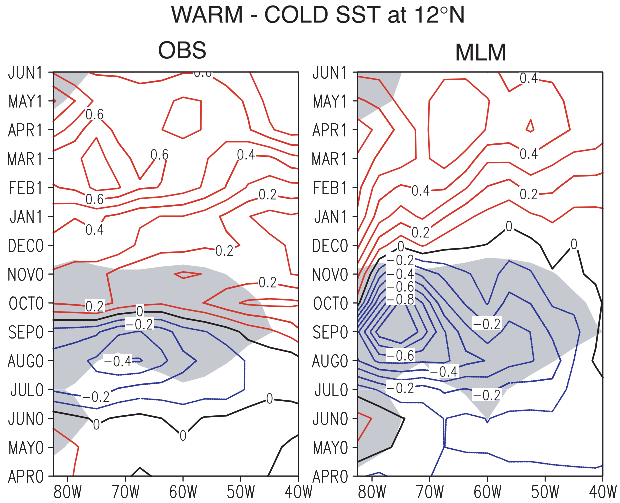

Figure 3. The composite El Niño - La Niña SST (contour interval 0.1°C) along 12°N in the Atlantic from April (0) to June (1) from observations and the MLM. Positive (negative) contours are red (blue), zero line is black. Shading indicates where the climatological monthly mean SST exceeds 28°C.

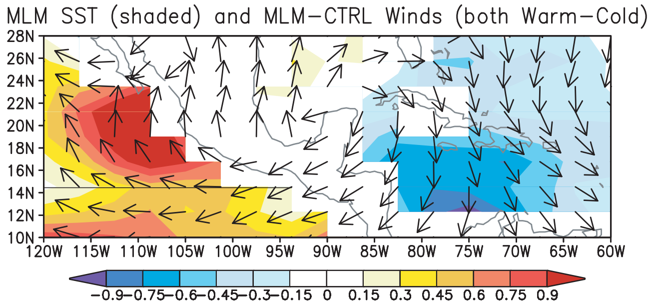

Figure 4. The composite El Niño - La Niña SST (shaded) during September (0) in the MLM. Vectors show the difference between the anomalous (El Niño - La Niña) surface wind direction in the MLM minus the Control experiment. Pacific SSTs south of the line at 15°N are specified.

departures (′) from the mean (the ‾ and ′ values are computed from the individual simulations and then ensemble averaged), we can assess the impact of deviations in U and ΔT and Δq on Q_{sh} and Q_{lh}. Both $U'\overline{\Delta q}$ and $\overline{U}\Delta q'$ contribute to Q_{lh} anomalies that warm the subtropical north Atlantic during DJF (not shown). However, the $U'\overline{\Delta q}$ component is dominant in the tropics and subtropics and is approximately twice as large as $\overline{U}\Delta q'$ in the eastern Caribbean where both reach a maximum. The covariance term, $U'\Delta q' - \overline{U'\Delta q'}$, is negligible. The relative contribution of the fluxes associated with temperature and moisture anomalies increase with latitude, such that $U'(\overline{\Delta T} + \overline{\Delta q})$ and $\overline{U}(\Delta T' + \Delta q')$contribute about equally to $Q_{sh} + Q_{lh}$ anomalies in the Gulf of Mexico while the latter dominate north of ~35°N. These findings are consistent with *Cayan* [1992], *Halliwell and Mayer* [1996] and *Alexander and Scott* [1997] who found that U' is essential for generating SST anomalies in the tropics while $\Delta T'$ and $\Delta q'$ are more important at mid and high latitudes.

[10] The observed and simulated composites of SST anomalies across the Atlantic basin along 12°N are shown in Figure 3. The warm SST anomalies, discussed above and in previous studies, form at the end of year(0) and continue through Jun(1). They are preceded by negative anomalies in the summer and early fall of year(0). We are uncertain why the latter are of larger amplitude and peak one month later in the model compared with observations. In the MLM experiment, anomalously cold water extends over the Caribbean and the eastern subtropical Atlantic during September (SEP 0) (Figure 4), when the climatological monthly mean SSTs are maximized (Figure 3). These negative SST anomalies are primarily due to Q_{lh} anomalies, although Q_{sw} also cools the ocean between 15°N–20°N (not shown).

[11] During Sep(0) the ENSO signal in the MLM experiment includes high pressure and reduced precipitation over Central America and the Gulf of Mexico/western Caribbean Sea (Figure 5, top). We examine the influence of air-sea interaction outside the tropical Pacific on these anomalies by comparing the MLM with the Control experiment. Differences between the two are collocated and in phase with the ENSO signal itself: the pressure is higher and the precipitation lower over Central America in the MLM compared with the Control (Figure 5, bottom). The magnitude of the difference is on the order of 40% of the original ENSO-related anomalies. Monte Carlo methods [*Livezey and Chen*, 1983] indicate that the difference between MLM and Control composites are field significant at the 95% level. These results suggest that the SST anomalies that form in the Caribbean in late summer/early

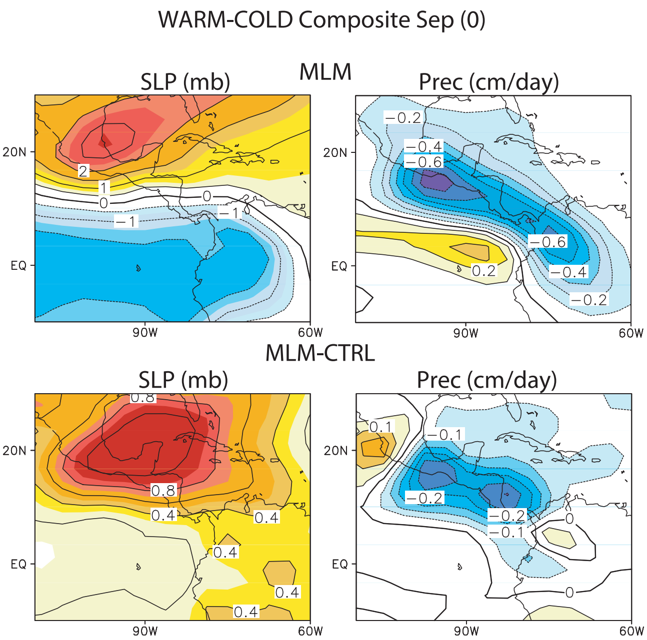

Figure 5. The composite El Niño - La Niña SLP (mb) and precipitation (cm day^{-1}) during September (0) in the MLM (top panels) and in the MLM minus the Control experiment (bottom panels). The contour interval for SLP is 0.5 (0.2) and the precipitation interval is 0.1 (0.05) in the top (bottom) panels.

fall have a substantial positive feedback on the original ENSO signal.

4. Discussion

[12] The extent to which SST anomalies influence the atmosphere is likely to depend on the base state, especially the mean seasonal cycle of SSTs. For example, the relatively large ENSO-related SST anomalies that occur in the tropical Atlantic and Gulf of Mexico in boreal spring have a negligible influence on the atmosphere as indicated by the difference in the MLM and Control experiments (not shown). The mean SSTs in spring are less than 27°C, and thus do not favor convection. In contrast, the Caribbean SST anomalies in fall are relative to a very warm base state and (> 28.5°C) where modest SST anomalies can induce large changes in convection [*Graham and Barnett*, 1987]. Indeed, relative to the Control, there is enhanced low-level divergence in the MLM experiment over the anomalously cold waters north of South America in Sep(0) (not shown). However, the response of the atmosphere to the developing SST anomalies is likely influenced by land-sea contrasts and the topography of the surrounding continents, i.e. the MLM-Control differences in precipitation are not maximized directly above the SST anomalies but downstream over Central America (Figures 4 and 5). SST anomalies near 20°N in the far eastern Pacific are associated with onshore flow and enhanced precipitation over the adjacent section of Mexico in the MLM relative to the Control simulations. The model results are consistent with the observational analyses of *Enfield and Alfaro* [1999] and *Giannini et al.* [2000] who found that Central American precipitation is related to SST anomalies of opposite sign in the tropical Pacific Ocean and the Caribbean Sea during ENSO events.

[13] *Wang and Enfield* [2001] found observational evidence for positive air-sea feedback in the "Western Hemisphere warm pool" (WHWP - defined as the region where SSTs are > 28.5°C), which extends over the Gulf of Mexico, Caribbean Sea and eastern north Pacific during summer and fall. They also found that the size of the WHWP and the SST anomalies within it are influenced by ENSO. Wang and Enfield suggested that atmosphere-ocean feedback in the WHWP occurs through long wave radiation. However, a comparison of the ENSO signal in MLM and Control experiments indicated that the feedback was primarily through Q_{lh}; differences between Q_{lw} anomalies in the two experiments were negligible. *Carton et al.* [1996], *Chang et al.* [1997], and *Xie and Tanimoto* [1998] also found that evaporation ($\propto Q_{lh}$) is critical to positive air-sea feedback in the tropical Atlantic; furthermore, *Chang et al.* [2000] found that the feedback primarily occurs in the WHWP. These studies indicated that the feedback occurs through changes in $U'\overline{\Delta q}$, but our experiments indicated that the *summertime* SST anomalies are both generated and influenced by $\overline{U}\Delta q'$ (not shown). In addition, air-sea interaction in the WHWP did not result in a local positive atmosphere-to-ocean feedback, as hypothesized by *Chang et al.* [1997], since Q_{lh} anomalies in the MLM are weaker and of shorter duration than those in the Control over the ENSO cycle (not shown). While our results suggest that changes in the WHWP influence the moisture available for convection over the nearby landmass, the processes responsible for these changes are not yet clear and maybe very sensitive to the physical parameterizations used in the model.

[14] **Acknowledgments.** We thank John Lanzante at GFDL for performing the model experiments used in this study and the reviewers whose suggestions greatly improved the manuscript.

References

Alexander, M. A., and J. D. Scott, Atlas of Climatology and variability in the GFDL R30S14 GCM, *U. S. Government Printing Office*: 1996–774–842, pp. 121, 1996.
Alexander, M. A., and J. D. Scott, Surface flux variability over the North Pacific and North Atlantic Oceans, *J. Climate*, *10*, 2963–2978, 1997.
Alexander, M. A., I. Blade, M. Newman, J. R. Lanzante, N. C. Lau, and J. D. Scott, The atmospheric bridge: the influence of ENSO teleconnections on air-sea interaction over the global oceans, *J. Climate*, in press, [available from http://www.cdc.noaa.gov/~maa/publications.shtml], 2002.
Carton, J. A., X. Cao, B. S. Giese, and A. M. da Silva, Deadal and interannual SST variability in the tropical Atlantic, *J. Phys. Oceanogr.*, *26*, 1165–1175, 1996.
Cayan, D. R., Variability of latent and sensible heat fluxes estimated using bulk formulae, *Atmos.-Ocean*, *30*, 1–42, 1992.
Chang, P. R., L. Ji, and H. Li, A decadal climate variation in the tropical Atlantic Ocean from thermodynamic air-sea interactions, *Nature*, *385*, 516–518, 1997.
Chang, P., R. Saravanan, L. Ji, and G. C. Hegerl, The effect of local sea surface temperatures on atmospheric circulation over the tropical Atlantic sector, *J. Climate*, *13*, 2195–2216, 2000.
Covey, D. L., and S. Hastenrath, The Pacific El Niño phenomenon in the Atlantic Sector, *Mon. Wea. Rev.*, *106*, 1280–1287, 1978.
Curtis, S., and S. Hastenrath, Forcing of anomalous sea surface temperature evolution in the tropical Atlantic during Pacific warm events, *J. Geophys. Res.*, *100*, 15,835–15,847, 1995.
Enfield, D. B., and D. A. Mayer, Tropical Atlantic sea surface temperature variability and its relation to El Niño-Southern Oscillation, *J. Geophys. Res.*, *102*, 929–945, 1997.
Enfield, D. B., and E. J. Alfaro, The dependence of Caribbean rainfall on the interaction of the tropical Atlantic and Pacific Oceans, *J. Climate*, *7*, 2093–2103, 1999.
Giannini, A., Y. Kushnir, and M. A. Cane, Interannual variability of Caribbean rainfall, ENSO and the Atlantic Ocean, *J. Climate*, *13*, 297–311, 2000.
Graham, N. E., and T. P. Barnett, Sea surface temperature, surface wind divergence and convection over the tropical oceans, *Science*, *238*, 657–659, 1987.
Halliwell, G. R., and D. A. Mayer, Frequency response properties of forced climatic SST anomaly variability in the North Atlantic, *J. Climate*, *9*, 3575–3587, 1996.
Harrison, D. E., and N. K. Larkin, El Niño-Southern Oscillation sea surface temperature and wind anomalies, *Rev. Geophys.*, *36*, 353–399, 1998.
Klein, S. A., B. J. Soden, and N.-C. Lau, Remote sea surface variations during ENSO: evidence for a tropical atmospheric bridge, *J. Climate*, *12*, 917–932, 1999.
Livezey, R. E., and W. Y. Chen, Statistical field significance and its determination by Monte Carlo techniques., *Mon. Wea. Rev.*, *111*, 46–59, 1983.
Mestas-Nuñez, A. M., and D. B. Enfield, Eastern equatorial Pacific SST variability: ENSO and non-ENSO components and their climatic associations, *J. Climate*, *14*, 391–402, 2001.
Saravanan, R., and P. Chang, Interaction between tropical Atlantic variability and El Niño-Southern Oscillation, *J. Climate*, *13*, 2177–2194, 2000.
Trenberth, K. E., The Definition of El Niño, *Bull. Amer. Meteor. Soc.*, *78*, 2562–2584, 1997.
Wang, C., and D. B. Enfield, The tropical Western Hemisphere warm pool, *Geophys. Res. Lett.*, *28*, 1635–1638, 2001.
Xie, S.-P., and Y. Tanimoto, A pan-Atlantic decadal climate oscillation, *Geophys. Res. Lett.*, *25*, 2185–2188, 1998.

M. Alexander and J. Scott, NOAA-CIRES Climate Diagnostics Center, R/CDC1, 325 Broadway, Boulder, Colorado 80305-3328, USA. (maa@cdc.noaa.gov)